Biomaterials 259 (2020) 120283

Contents lists available at ScienceDirect

Biomaterials

journal homepage: www.elsevier.com/locate/biomaterials

Bile canaliculi contract autonomously by releasing calcium into hepatocytes via mechanosensitive calcium channel

Kapish Gupta [a], Inn Chuan Ng [b], Gowri Manohari Balachander [b], Binh P. Nguyen [c], Lisa Tucker-Kellogg [d], Boon Chuan Low [a,e,f,**], Hanry Yu [a,b,f,g,h,i,*]

[a] Mechanobiology Institute, National University of Singapore, T-Lab, 5A Engineering Drive 1, 117411, Singapore
[b] Department of Physiology, Yong Loo Lin School of Medicine, 2 Medical Drive, 117593, Singapore
[c] School of Mathematics and Statistics, Victoria University of Wellington, New Zealand
[d] Cancer and Stem Cell Biology, and Centre for Computational Biology, Duke–NUS Medical School, Singapore
[e] Department of Biological Sciences, National University of Singapore, Singapore
[f] University Scholars Programme, National University of Singapore, 138593, Singapore
[g] Institute of Bioengineering and Nanotechnology, A*STAR, The Nanos, #04-01, 31 Biopolis Way, 138669, Singapore
[h] CAMP, Singapore-MIT Alliance for Research and Technology, 1 CREATE Way, Level 4 Enterprise Wing, 138602, Singapore
[i] Department of Gastroenterology, Nanfang Hospital, Southern Medical University, Guangzhou, China

ARTICLE INFO

Keywords:
Piezo
Canalicular pressure
Bile canaliculi derived vesicles
Hepatocellular cholestasis
Mechanosensitive ion channels
Liver disease

ABSTRACT

Drug-induced hepatocellular cholestasis leads to altered bile flow. Bile is propelled along the bile canaliculi (BC) by actomyosin contractility, triggered by increased intracellular calcium (Ca^{2+}). However, the source of increased intracellular Ca^{2+} and its relationship to transporter activity remains elusive. We identify the source of the intracellular Ca^{2+} involved in triggering BC contractions, and we elucidate how biliary pressure regulates Ca^{2+} homeostasis and associated BC contractions. Primary rat hepatocytes were cultured in collagen sandwich. Intra-canalicular Ca^{2+} was measured with fluo-8; and intra-cellular Ca^{2+} was measured with GCaMP. Pharmacological modulators of canonical Ca^{2+}-channels were used to study the Ca^{2+}-mediated regulation of BC contraction. BC contraction correlates with cyclic transfer of Ca^{2+} from BC to adjacent hepatocytes, and not with endoplasmic reticulum Ca^{2+}. A mechanosensitive Ca^{2+} channel (MCC), Piezo-1, is preferentially localized at BC membranes. The Piezo-1 inhibitor GsMTx-4 blocks the Ca^{2+} transfer, resulting in cholestatic generation of BC-derived vesicles whereas Piezo-1 hyper-activation by Yoda1 increases the frequency of Ca^{2+} transfer and BC contraction cycles. Yoda1 can recover normal BC contractility in drug-induced hepatocellular cholestasis, supporting that Piezo-1 regulates BC contraction cycles. Finally, we show that hyper-activating Piezo-1 can be exploited to normalize bile flow in drug-induced hepatocellular cholestasis.

1. Introduction

Drug-induced hepatocellular cholestasis causes cellular toxicity, liver injury, and can even lead to acute liver failure [1,2]. In healthy liver function, bile acids (BA) are transported into the bile canaliculi (BC) by ATP-dependent export pumps [3], and then propelled from the BC to the intra-hepatic bile ducts by BC contractions [4]. These two transport mechanisms work coherently to expel bile from the canaliculi. Any defect in either can lead to BA build-up in the hepatocytes or in the BC lumen, leading to cholestasis [5]. There have been reports of reduced lumenal contractility under conditions that alter transporter activity [6]. However, the relationship between the transporter activity and BC contractility is not well understood [5]. This gap in understanding BC contractility has impeded development of effective drugs to manage hepatocellular cholestasis, and thus we aim at unraveling the regulatory mechanism of BC contractions.

The BC lumenal structure is supported by an actin-rich filamentous cytoskeleton, the peri-canalicular actin cortex (PAC). BC contraction is

Abbreviations: BA, Bile acid; BC, Bile canaliculi; BCV, Bile canaliculi derived vesicles; Ca^{2+}, Calcium; ER, endoplasmic reticulum; ICP, intra-canalicular pressure; MCC, mechanosensitive Calcium channel; PAC, peri-canalicular actin cortex; tbuHBQ, 2,5-di-(ter-butyl)-1,4-benzohydroquinone; GB, glyburide; KTZ, Ketoconazole.

* Corresponding author. 04-11, MD 9, 2 Medical Drive, National University of Singapore, 117597, Singapore.
** Corresponding author. Mechanobiology Institute, National University of Singapore, T-Lab, 5A Engineering Drive 1, 117411, Singapore.
E-mail addresses: dbslowbc@nus.edu.sg (B.C. Low), hanry_yu@nuhs.edu.sg (H. Yu).

https://doi.org/10.1016/j.biomaterials.2020.120283
Received 24 February 2020; Received in revised form 17 June 2020; Accepted 1 August 2020
Available online 11 August 2020

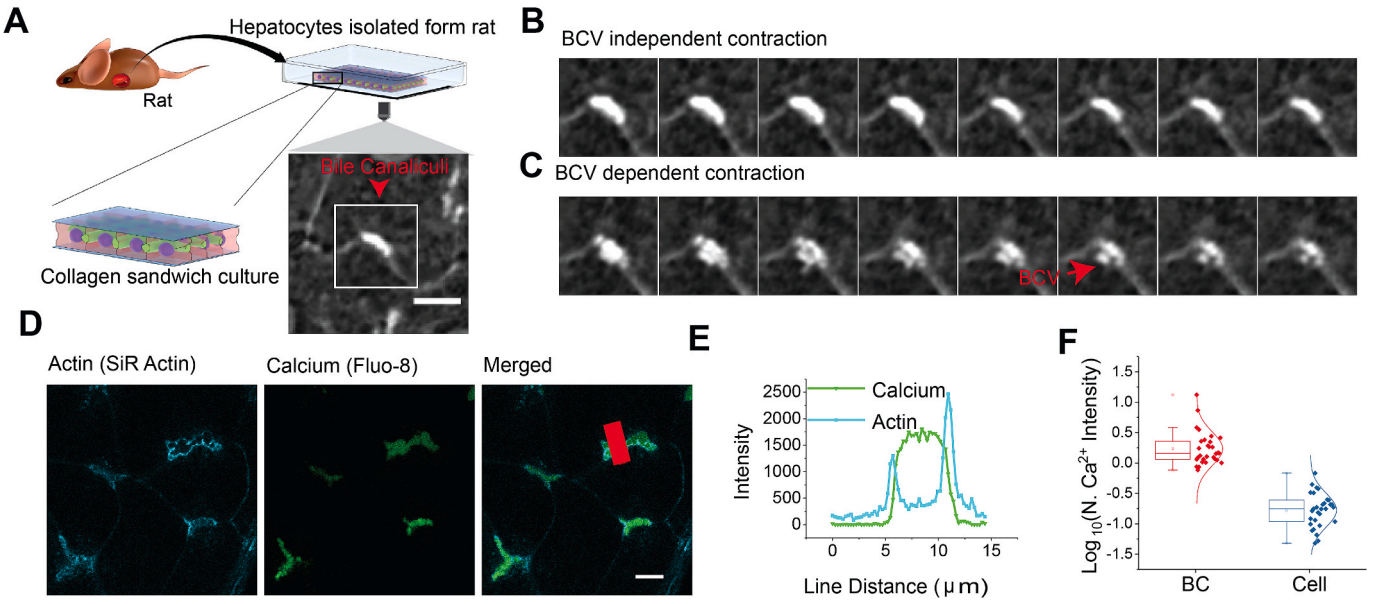

Fig. 1. Visualizing BC contractions in primary rat hepatocytes and Ca^{2+} in BC. (A) Schematic showing isolation of hepatocytes and collagen sandwich culture. Time-lapse phase-contrast images of two different BCs undergoing BCV-independent (B) and BCV-dependent contractions (C). (D) A representative image showing live Ca^{2+} imaging in cells with Fluo-8 (green). Actin was stained using SiR-Actin (cyan). Scale bar represent 10 μm. (E) Plot of Ca^{2+} and Actin intensity across the red box drawn in (D). (F) Quantification of Ca^{2+} intensity in BC and in the cells surrounding the BC (N = 30, 3 independent experiments). (For interpretation of the references to color in this figure legend, the reader is referred to the Web version of this article.)

regulated by contraction of the PAC [7], which is induced by a surge in intra-cellular calcium (Ca^{2+}) [8]. Yet, the source of the intra-cellular Ca^{2+} is still debated. Studies have suggested that extracellular hormones stimulate IP3-dependent release of endoplasmic reticulum (ER) Ca^{2+} [9,10] to trigger BC contractions. However, primary hepatocytes exhibit BC contractions periodically, *in vitro,* in the absence of hormones. Furthermore, multiple non-hormonal triggers have shown to increase intracellular Ca^{2+} and lead to BC contractions [11]. In our previous study, we observed that inter-canalicular pressure (ICP), caused by increases in lumenal contents, could cause contractility in the PAC and contractions of the BC lumen [12].

We hypothesize that BC is an autonomous contractile unit that regulates its own contractions by coupling the ICP to Ca^{2+} trafficking through mechanosensitive Ca^{2+} channels (MCC) on the BC membrane. We identified Piezo-1 as the MCC through which intra-BC Ca^{2+} regulates the BC contractions, and we showed that modulation of Piezo-1 activities was sufficient to normalize bile flow in a model of drug-induced hepatocellular cholestasis.

2. Materials and methods

Isolation and culture of rat hepatocytes: Hepatocytes were isolated from male Wistar rats (weighing 200–300 g, obtained from InVivos, Singapore) via two-step collagenase perfusion. Animals were handled in accordance to the Institutional Animal Care and Use Committee (IACUC) protocol (Protocol Number: R15–0027) approved by the IACUC of the National University of Singapore (NUS). Approximately 300 million cells were isolated per rat, with >90% viability as determined by Trypan blue exclusion assay. Isolated hepatocytes were cultured in collagen sandwich as described in Supplementary Data.

Intracellular Ca^{2+} Measurements: Hepatocytes were transfected with GCaMP as described in Supplementary Data. The Ca^{2+} dynamics in labeled cells were monitored by confocal (Nikon A1R), and time-lapse images were captured at 1–2 s time intervals for 5–10 min. Images were analyzed as described in Image Analysis section in Supplementary Data.

Labelling Hepatocytes with Ca^{2+} dyes: Multiple Ca^{2+} dyes were screened to image Ca^{2+} in hepatocytes as per manufacturer's protocol. Fluo-8 was primarily used in all the experiments as it was most stable for long-term imaging. Hepatocytes were cultured in collagen sandwich for 40 h, after which media was changed to 1 mL fresh William's E media (containing 4 μM Fluo-8) and incubated for 30 min. Following incubation, the cells were imaged at 30 s intervals for 40 min using Nikon IMQ at 20× magnification. To examine the effects of inhibition/activation of various canonical Ca^{2+} channels, channel inhibitors/activators such as 2,5-di-(ter-butyl)-1,4-benzohydroquinone (tbuHBQ), Thapsigargin, A23187, Cyclopiazonic acid, Xestospongin C, Yoda-1, Glyburide (GB), Ketoconazole (KTZ) or GsMTx-4, were added along with Fluo-8 as described in Supplementary Data.

Image Analysis: X–Y drift (if any) was corrected in IMARIS and corrected images were further processed either using MATLAB, Fiji or IMARIS as described in Supplementary Data. The Ca^{2+} fluctuations inside BC were represented as kymographs based on a line drawn in the middle of BC. Most of the kymographs were calculated over 40 min unless otherwise stated. The 'Integrated Ca^{2+} intensity' was calculated by measuring the Ca^{2+} intensity over the maximum projected area for all the frames captured. This was used to describe the total Ca^{2+} in the BC and is sensitive to the changes in the area and Ca^{2+} levels in BC. The 'Line Ca^{2+} intensity' was the Ca^{2+} intensity measured across the line in the kymograph and was sensitive to the drop in the BC Ca^{2+} levels. Unless otherwise stated, we quantified data from 15 BC, 5 each from three independent experiments. All the graphs tracing 'Ca^{2+} intensity' and 'BC Area' versus time are representative graphs under the conditions specified. Furthermore, we have shown data as kymographs, where each kymograph represents an individual BC, and unless otherwise, stated we have shown 6 kymographs (2 each from three independent experiments). Additional image analysis is described in Supplementary Data.

Statistical Analysis: Data are presented as mean ± standard error of the mean (SEM). In most groups, the initial test of difference across groups was analyzed using one-way ANOVA. The Student's *t*-test was then used as a post-hoc test to identify the significant differences among the different experimental conditions. p values < 0.05 (*), $p < 0.01$ (**) were considered statistically significant. For testing significance of change in slope with Ca^{2+} wave, sign test was also used to analyze the significance of the reduction in BC area.

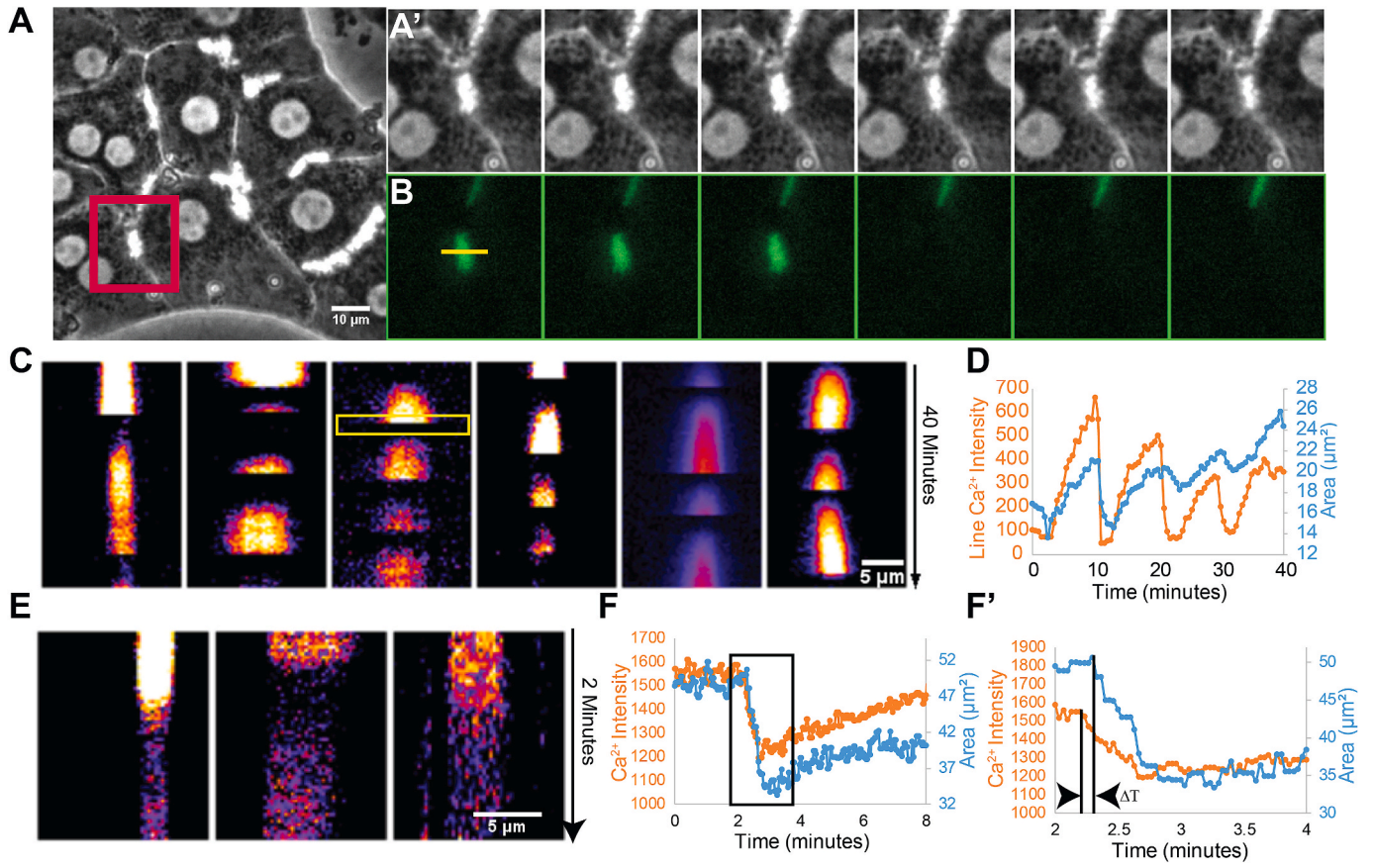

Fig. 2. Ca^{2+} level fluctuates in BC and the BC Ca^{2+} level drops prior to BC contraction. (A) Phase-contrast live imaging of primary rat hepatocytes. Fluo-8 was used to stain Ca^{2+}. Representative time-lapse images (30 s interval) of a BC indicated by red box in (A) is shown in (A′) and the corresponding Fluo-8 fluorescent images are shown in (B). Ca^{2+} intensity fluctuations for six different BCs from three different experiments are shown as kymographs in (C). The third kymograph is drawn across the yellow line in (B), and the yellow box highlights kymograph for time lapse shown in (B). (D) Representative graph for BC line Ca^{2+} intensity and the BC area, measured simultaneously over a period of 40 min. (E) Kymographs from three different BCs for Ca^{2+} intensity measured at 1–3 s intervals over a period of 2 min are shown. (F) Representative graph of BC line Ca^{2+} intensity and the BC area, measured at 1–3 s intervals over a period of 8 min. The boxed region in (F) has been digitally resolved and represented in (F′). The arrowheads indicate ~10 s delay (ΔT) between the drop in BC Ca^{2+} intensity and the drop in BC area. We observed around 10.37 ± 1.17 s delay between the drop in BC Ca^{2+} intensity and the drop in BC area (N = 12 BC, 6 independent experiments). (For interpretation of the references to color in this figure legend, the reader is referred to the Web version of this article.)

3. Result

3.1. Ca^{2+} is concentrated in BC

Primary rat hepatocytes were cultured in collagen sandwiches to form BC, which appear as bright tube-like structures [13] along the cell-cell interface (Fig. 1A). BC are dynamic structures that expand and contract periodically (Supporting Video 1) [7,14–17]. BC contractions were observed as a decrease in the BC area without (Fig. 1B) or with the formation of blebs or BC-derived vesicles (BCV) (Fig. 1C). Here we have focused on BCV-independent contractions, which account to 80–90% of BC contractions in sandwich culture [12]. To identify the source of Ca^{2+} that led to BC contractions, we treated primary rat hepatocytes with fluorescent-based Ca^{2+} indicators, Calcium Green™-1 AM, Fluo-4 and Fluo-8. Live fluorescent imaging showed that Ca^{2+} was concentrated inside the BC (Fig. 1D and Supporting Fig. 1A). To confirm that BC, not ER is the source of Ca^{2+}, we demarcated BC by staining for actin (SiR-Actin™) in cells and imaged the entire depth of BC. In a line intensity analysis across a BC (red line in Fig. 1D), high intensity actin peaks (BC boundary), flanked high intensity Ca^{2+} peak (Fig. 1E). 3D image reconstruction (supporting Video 2) confirmed Ca^{2+} localization inside BC (Supporting Fig. 1A–B), and not in the cytoplasmic side of the PAC. Furthermore, Ca^{2+} intensity in BC was a many fold higher than in the adjacent cells (Fig. 1F and supporting Fig. 1C). Live imaging of cells with high laser power led to phototoxicity. Hence low laser power was used to visualize BC Ca^{2+}, which precluded the detection of cytoplasmic Ca^{2+} (Supporting Figs. 1B and 2E-F). The high concentration of Ca^{2+} inside BC intrigued us and we hypothesized that the canalicular Ca^{2+} may play a role in BC contractions.

Supplementary video related to this article can be found at https://doi.org/10.1016/j.biomaterials.2020.120283

3.2. BC Ca^{2+} depletion triggers BC contraction

In order to dissect the role of Ca^{2+} in BC contractions, we performed high-resolution time-lapse imaging. Live-cell Ca^{2+} imaging with Fluo-8 at 30 s intervals indicates depletion of BC Ca^{2+} during BC contraction (Fig. 2A, B). Kymographs depicting changes in BC Ca^{2+} intensity over time showed periodic increase and decrease in BC Ca^{2+} (Fig. 2C). Concurrent tracing of BC Ca^{2+} intensity and BC area showed that the periodic decrease in BC Ca^{2+} was synchronous with the BC contractions (Fig. 2D, Supporting Fig. 1E–H and Supporting Video 3). To understand the temporal relationship between BC contraction and BC Ca^{2+} depletion, we imaged the BC Ca^{2+} fluxes and contractions at every 2 s for 5–10 min (Fig. 2E). BC Ca^{2+} depletion precedes every BC contraction (Fig. 2F), with a time difference of ~10 s (10.37 ± 1.17 s) between the initiation of the Ca^{2+} depletion and the initiation of BC contraction (Fig. 2F and Supporting Fig. 2A–B), suggesting that BC Ca^{2+} depletion

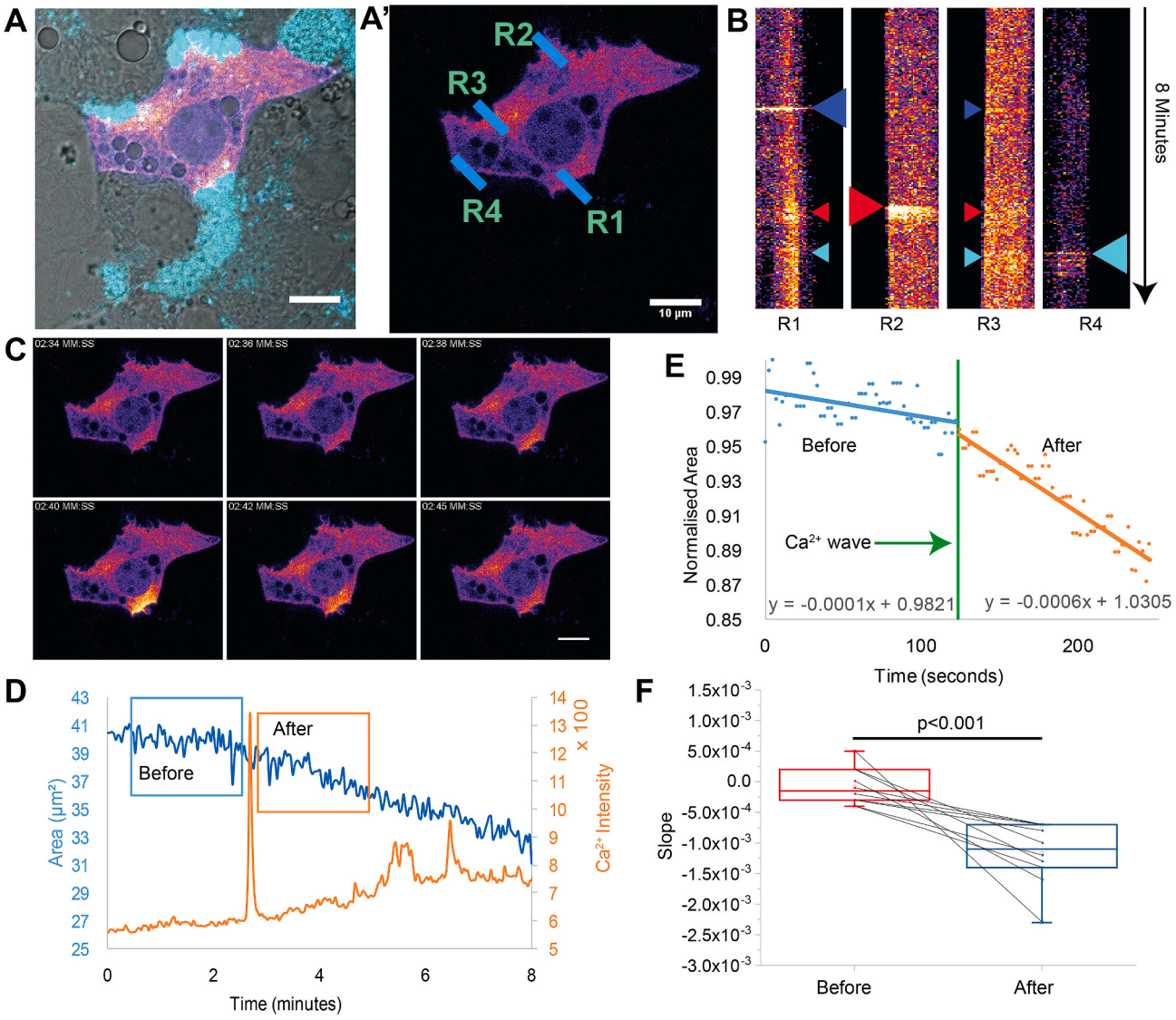

Fig. 3. Apical Ca^{2+} triggers BC contraction. Live Ca^{2+} imaging of hepatocytes transfected with GCaMP. (A) Hepatocyte with three BCs (marked in cyan), indicated by regions R1, R2 and R3 in (A′). The region R4 is along an intercellular junction. (B) Kymographs depicting Ca^{2+} intensities detected across the lines drawn over the four regions in (A′). The large arrowheads in R1 and R2 denote the increase in intracellular Ca^{2+} due to BC contractions in the respective regions. The small arrowheads indicate increase in Ca^{2+} in that region due to the Ca^{2+} waves emanating from BC contractions in other regions (indicated by the same color). The large cyan arrowhead in R4 depicts a low-intensity Ca^{2+} waves generated at the cell-cell interface. (C) Time-lapse images of the cell (2 s intervals) before and after the BC contraction at R1. (D) Graph of intracellular Ca^{2+} intensity and the BC area at R1. (E) Line fitted graph of the BC area from (D) before (blue box) and after (orange box) the Ca^{2+} surge. Similar measurements were performed for ten different BCs (5 independent experiments) and the slope of the normalized area are plotted in (F). All scale bars represent 10 μm. (For interpretation of the references to color in this figure legend, the reader is referred to the Web version of this article.)

might cause or trigger BC contractions.

Supplementary video related to this article can be found at https://doi.org/10.1016/j.biomaterials.2020.120283

3.3. Ca^{2+} waves in hepatocytes are associated with BC contractions

We observed a slight increase in the cytoplasmic Ca^{2+} in the cells forming the BC lumen, concurrently with the BC Ca^{2+} depletion (Supporting Fig. 2C, D′), suggesting that BC Ca^{2+} was transported into the adjacent cells during contractions. Due to low signal to background ratio, cytotoxicity, and photobleaching, we found Fluo-8 to be unsuitable for live intracellular Ca^{2+} imaging (Supporting Fig. 2E and F) and transfected a Ca^{2+} sensor GCaMP [18] into primary rat hepatocytes (Fig. 3A). We traced the changes in intracellular Ca^{2+} in individual GCaMP-transfected cells and observed that the increase in Ca^{2+} intensity following a BC contraction spread to the distal regions of the cell within 2–8 s. This wave, originating at the apical, BC-forming side of the cell (Supporting Fig. 3A, large arrowhead) decreased in intensity as it travelled through the cell (Supporting Fig. 3A, small arrowhead). In Fig. 3 we annotate a cell that borders three BCs and one cell-cell junction (at regions marked R1, R2, R3, R4, respectively) (Fig. 3A'). We traced Ca^{2+} intensities in these regions for 8 min (Fig. 3B and C). The high intensity Ca^{2+} wave at R1 at 2 min 40 s was associated with BC contraction (Fig. 3D, decrease in BC area). However the low intensity waves at 5 min 40 s and 6 min 30 s did not synchronize with any BC contractions. While most Ca^{2+} waves originated at the BC interface, we also observed some Ca^{2+} waves originating from cell-cell contacts (R4 in Fig. 3B). We suspect that these non-BC Ca^{2+} waves originate from Ca^{2+} transfer across gap junctions. The non-BC waves showed no temporal association with the BC contractions (Supporting Fig. 3C, and supporting video 4). We line fitted the measurements for BC area with time before and after the intracellular Ca^{2+} spike and observed a rapid decrease in area following

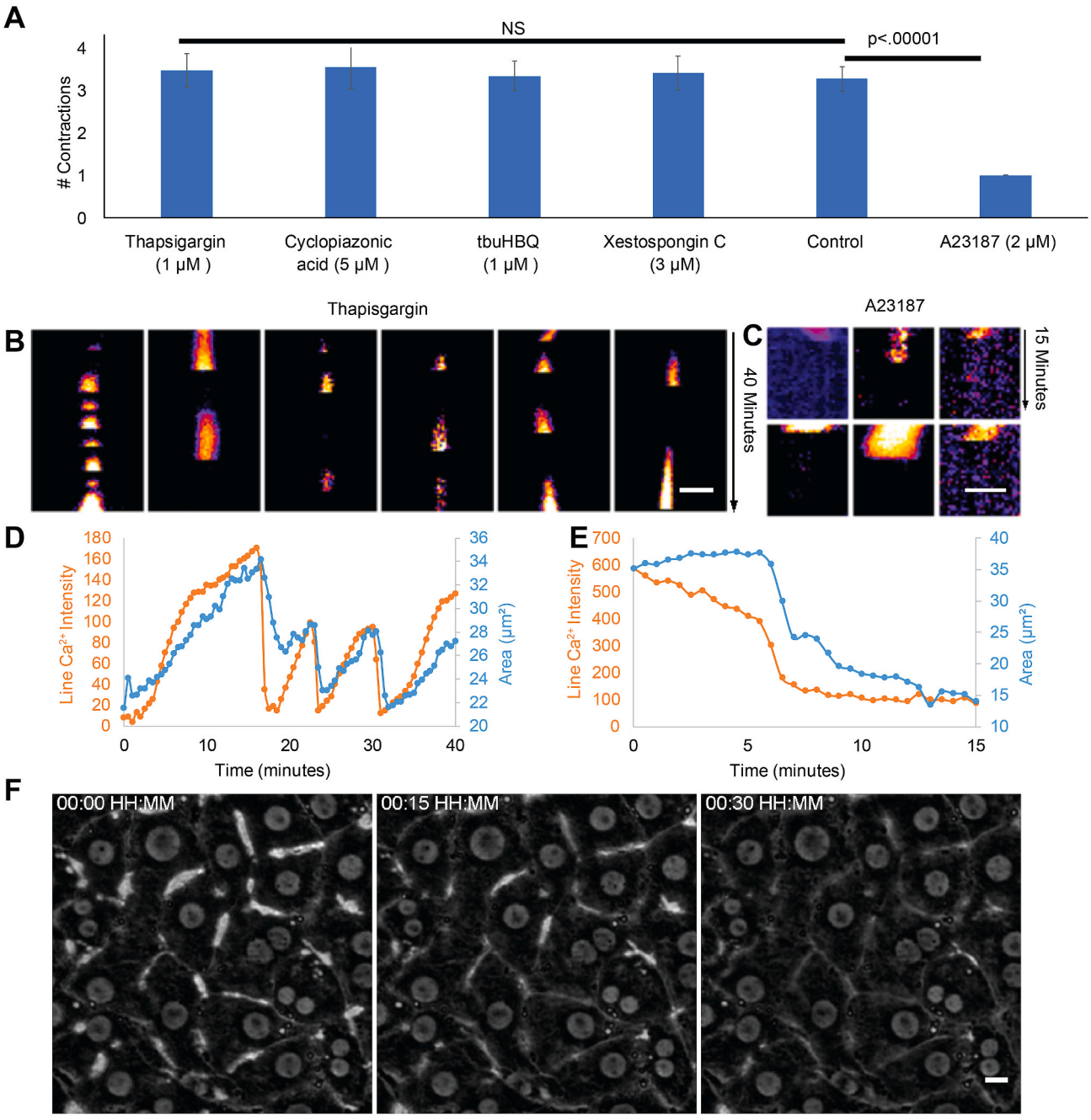

Fig. 4. BC contraction and BC Ca^{2+} cycles are independent of the ER Ca^{2+}. (A) Quantification of the number of BC contractions over a period of 40 min with the treatment of various ER and IP3 inhibitors and A23187 (N = 15, five each from three independent experiments). (B) and (C) show kymographs of BC line Ca^{2+} intensity with the treatment of Thapsigargin (40min) and A23187 (15 min) respectively (n = 6). (D) and (E) are representative graphs for BC line Ca^{2+} intensity and the BC area under conditions in (B) and (C) respectively (quantification in 4A, N = 15, five each from three independent experiments). (F) Time-lapse phase-contrast images of cells treated with A23187 showing a massive contraction which does not recover after 30 min. Scale bars in (B) and (C) represent 5 μm and in (F) represent 10 μm.

the Ca^{2+} spike (Fig. 3E). Similar trends were observed for ten different BCs (Fig. 3F). These observations support the hypothesis that BC Ca^{2+} transfer into the adjacent cells triggers BC contractions.

Supplementary video related to this article can be found at https://doi.org/10.1016/j.biomaterials.2020.120283

3.4. BC contracts independently of the Ca^{2+} release from ER

ER is the largest Ca^{2+} reservoir in eukaryotic cells and maintains the Ca^{2+} homeostasis [19]. It has been reported [9] that apico-basal Ca^{2+} waves in hepatocytes might be due to the Ca^{2+} release from ER (which surrounds BC) and IP3 generation in response to growth factors [20]. We investigated whether ER plays a role in regulating Ca^{2+} and BC contractions. We imaged the BC Ca^{2+} and contractions in the presence of multiple ER inhibitors (Fig. 4A) such as Thapsigargin (Fig. 4B and D) [21,22], Cyclopiazonic acid [23,24] (Supporting Fig. 5C and D) and tbuHBQ (Supporting Fig. 5E and F) [25]. Thapsigargin is a specific and potent inhibitor of sarco/endoplasmic reticulum Ca^{2+}-ATPase. It forms a dead-end complex with sarco/endoplasmic reticulum Ca^{2+}-ATPase and depletes ER Ca^{2+} causing increase in intracellular Ca^{2+} (Supporting Fig. 4). Cyclopiazonic acid competes with the ATP-binding site in sarco/endoplasmic reticulum Ca^{2+}-ATPase and leads to ER Ca^{2+} depletion,

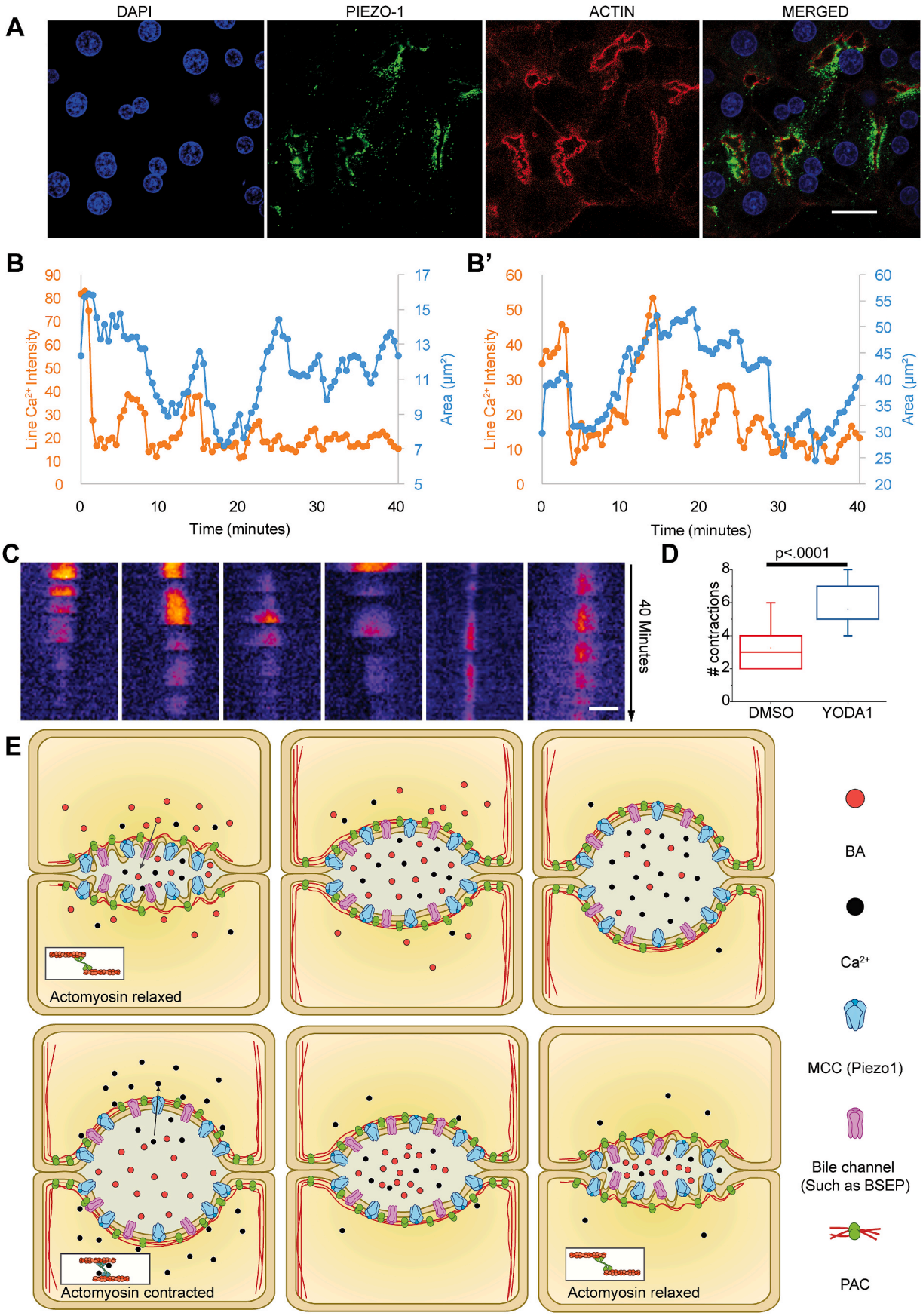

(caption on next page)

Fig. 5. MCC Piezo-1 conducts Ca^{2+} transport and mediates BC contractions. (A) Representative image showing Immunostaining of Piezo-1 (green) in hepatocytes on collagen sandwich culture. Actin is stained by Phalloidin (red). The nuclei are counterstained with Hoecsht (blue). Piezo-1 staining is localized at BC membrane and adjoining apical area, Piezo-1 also staines various small vesicles around BC. Also, Piezo-1 staining in not continuous over entire BC membrane and it appears in patches, this is probably due to Piezo-1 localization in plasma memnbrane regions associated with lipid rafts. (B) and (B′) show representative graphs depicting BC line Ca^{2+} intensity and the BC area from two sets of experiments wherein the cells were treated with Yoda-1. (C) Kymographs are shown for six BCs from three independent experiments under Yoda-1 treatment. (D) Quantification of BC contractions in cells treated with Yoda-1 and control (N = 15, five each from three independent experiments). (E) Schematic for the proposed model of BC contractions. BC is formed between adjacent hepatocytes and is surrounded by an actomyosin meshwork. BC contains transporter proteins, which transport various components of bile such as BA, bilirubin, ions and water from the cell into the lumen, leading to the expansion of BC. The expanding lumen increases the membrane tension and once a threshold is reached, Piezo-1 opens causing Ca^{2+} efflux from the BC into the cells. This Ca^{2+} interacts with the actomyosin network and initiates BC contraction. This cycle repeats in metabolically active hepatocytes under hoemostatic conditions. Scale bars in (A) and (C) represent 20 μm and 5 μm respectively. (For interpretation of the references to color in this figure legend, the reader is referred to the Web version of this article.)

whereas tbuHBQ blocks receptor-activated Ca^{2+} entry, leading to ER Ca^{2+} leakage [26]. BC contractions were unaffected by these drugs (Fig. 4A, average of 3 contractions in 40 min), with no changes in the BC Ca^{2+} cycles (Fig. 4B) and no changes in the temporal association of BC Ca^{2+} cycles with BC contractions (Fig. 4D). Similar results were obtained in the presence of 3 μM Xestospongin C (Supporting Fig. 5A and B) [27,28], a reversible IP3 receptor antagonist [29]. This suggests that BC contractions are independent of the ER Ca^{2+} store and sarco/endoplasmic reticulum Ca^{2+}-ATPase pump.

In the presence of 2 μM A23187, a Ca^{2+} ionophore (Supporting Fig. 4) [30,31], BC Ca^{2+} intensity rapidly decreased (Fig. 4C and E, drop in Line Ca^{2+} intensity before 5 min), followed by a BC contraction and collapse, which did not recover (Fig. 4F). The ionophore A23187 increases the permittivity of Ca^{2+} across cellular membranes and causes a surge in intracellular Ca^{2+}. It led to PAC contraction, and in the presence of the ionophore, the PAC remained contracted and the BC did not recover.

3.5. Piezo-1 acts as a tension sensor in BC

We find BC contractions areassociated with Ca^{2+} transport across BC. We then investigated the mechanism of Ca^{2+} transport across BC and its effects on BC contractions. Our previous work showed pressure (ICP) affects BC dynamics [12]. Hence we screened for MCCs that might control Ca^{2+} transport from BC to cells leading to BC contractions. We imaged the subcellular localization of four major MCCs such as, Piezo-1, Piezo-2, TRPC-4 and TRPC-6 (Supporting Fig. 6) [32], and only Piezo-1 is localized on the BC membrane (Fig. 5A and Supporting video 5). Piezo-1 is a Ca^{2+} channel that opens when the membrane pressure exceeds a threshold. Piezo-1 staining is localized at the BC membrane and adjoining apical areas. Piezo-1 also stains various small vesicles around the BC (Supporting Fig. 6). The positively stained membranes show patches of intensity, which would be consistent with Piezo-1 localization in plasma membrane regions associated with lipid rafts [33,34]. The diffuse Piezo-1 staining around BC made it difficult to perform robust colocalization studies (Supporting Fig. 6G). Thus, mere localization of Piezo-1 around BC was not enough to ascertain its role in BC dynamics.

Supplementary video related to this article can be found at https://doi.org/10.1016/j.biomaterials.2020.120283

To analyze if Piezo-1 can respond to the ICP, we imaged and quantified BC contractions in hepatocytes treated with Yoda-1, which activates Piezo-1 by reducing the pressure threshold at which Piezo-1 opens. The frequency of BC contractions increases in the presence of Yoda-1 (Fig. 5B–D), indicating that increased Piezo-1 activity leads to increased BC contractions. The maximum Ca^{2+} intensity observed during these BC contractions was lower (Fig. 5B and B') compared to untreated controls (Fig. 2D), suggesting that there may be a lower threshold ICP as a result of Yoda1-induced sensitization, leading to premature BC contractions.

We next inhibited the mechano-activation of Piezo-1 using GsMTx-4 [35]. Live Ca^{2+} imaging (with integrated and line Ca^{2+} intensity analysis) indicated no instances of Ca^{2+} depletion from the BC and no BC contraction cycles in the presence of GsMTx-4 (Fig. 6A–D). This contrasts with controls (Fig. 2D Kymographs), which showed periodic BC Ca^{2+} cycles. Quantification of the mean Ca^{2+} (measured as "line Ca^{2+} intensity") and BC area indicated that GsMTx-4 was sufficient to abrogate Ca^{2+} transport at the BC interface and halt BC contractions. This suggests that MCC activity is required for Ca^{2+} transport at the BC interface to cause BC contractions. It should be noted that there is a correlation between total BC area and total Ca^{2+} (Fig. 6B), but this may be inconsequential because bile is rich in Ca^{2+} and any non-contractile changes in BC area, such as pinching off BCV, must result in simultaneous changes in total BC volume and total BC Ca^{2+} (Fig. 6C). Inhibition of BC Ca^{2+} transfer to the adjacent cells halts BC contractions. This impairs the excretion of BC contents and causes elevation of ICP. In such cases, cells resort to relieve ICP through BCV. BCV formation is a cholestatic response due to increased ICP [12]. GsMTx-4 caused ~8-fold higher frequency of BCV (Fig. 6E), leading to a complete suppression of BCV-independent contractions [12]. Taken together, the effects of activation and inhibition of Piezo-1 indicate that Piezo-1 is required for transfer of BC Ca^{2+} to adjacent cells and BC contractions (Figs. 5E and 6F).

3.6. Piezo-1 activation rescues BC contractions inhibited by cholestatic drugs

We explore the modulation of BC contractions via modulating ICP. The transporters in the BC membrane secrete BA into the BC lumen and the increase in BC lumenal contents increases ICP. We hypothesize that decreasing ICP via BC-membrane transporter inhibition would inhibit BC contractions. We treated hepatocytes with 20 μM GB (MRP2 inhibitor [36]) and 12 μM KTZ (BSEP inhibitor [37]). Corroborating our hypothesis, the number of BC Ca^{2+} cycles was reduced (Fig. 7A and B) indicating that reduced transporter activity leads to impaired BC Ca^{2+} transport implicating lowered Piezo-1 activity. Concomitantly, reduction in BC contractions was observed (Fig. 7A, B, D). Since Piezo-1 hyper-activation can increase BC contractions (Fig. 5D), we then hypothesized that hyper-activating Piezo-1 under low ICP conditions should rescue the BC contractions. We hyper-activated Piezo-1 with Yoda-1 in cells treated with GB and KTZ and observed that the BC Ca^{2+} cycles (Fig. 7C) and the BC contractions (Fig. 7D,) were indeed rescued. The data indicate that drug-induced inhibition of transporters on the BC membrane reduced the BC contractions, and this reduction can be rescued by Peizo-1 hyperactivation. In summary, hyperactivation of Piezo-1 can rescue BC contractility and prevent the stasis of bile.

4. Discussion

Hepatocellular cholestasis is severely implicated in drug-induced liver injury and is one of the major reasons for drug withdrawal [37,38]. Hepatocellular cholestasis inducing drugs have been found to disrupt the activity of the transporters on the BC membrane, which cause BA build-up in the hepatocytes and reduced bile flow [5]. The effects of transporter inhibition on BC contraction-driven micro--peristalsis is unclear [4,14,30,39,40]. We elucidate the mechanism of BC contractions, which is critical to understand the normal BC physiology

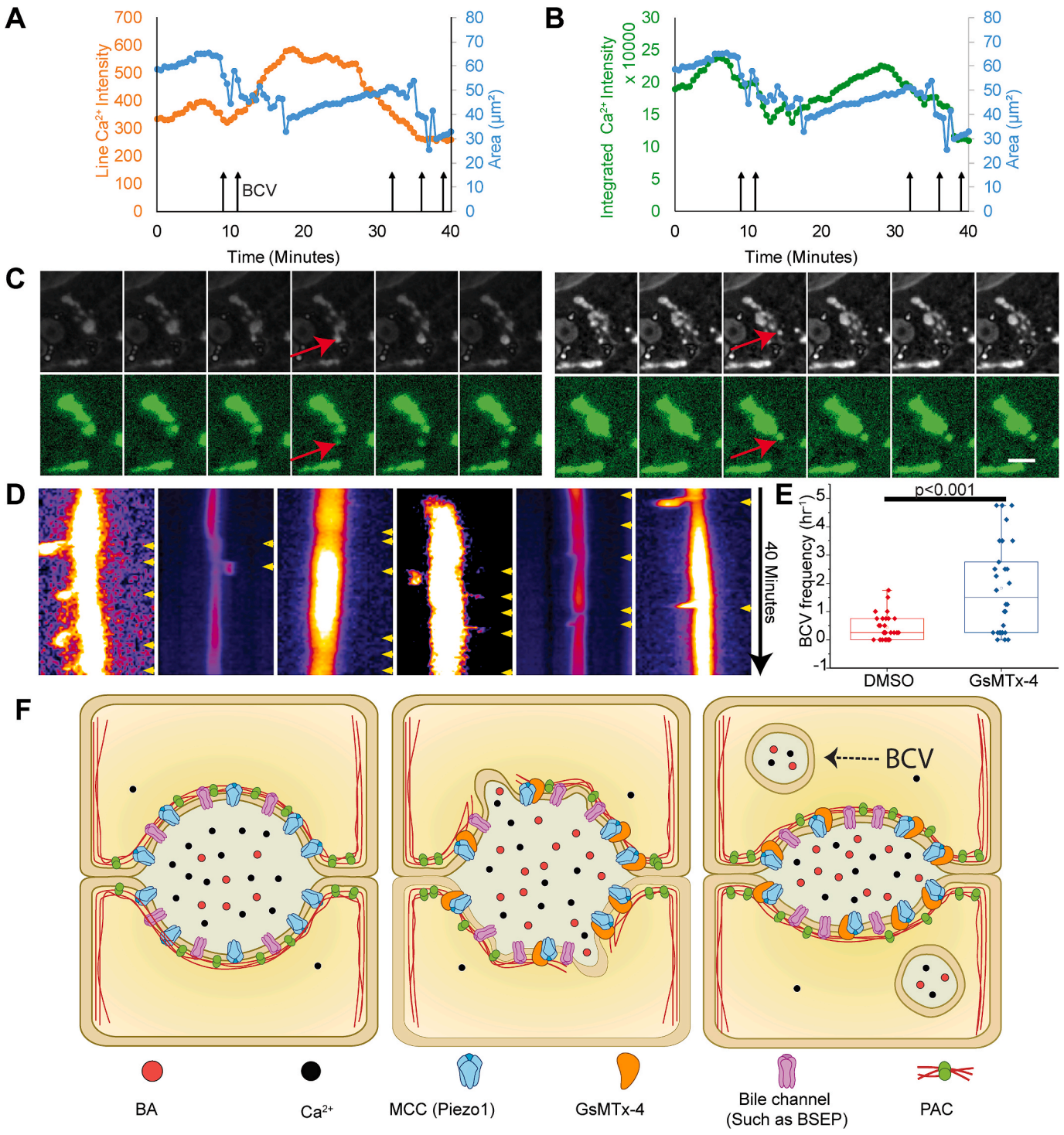

Fig. 6. Piezo-1 inhibition leads to BCV induction. Representative graphs for BC line Ca^{2+} intensity versus BC area (A) and BC integrated Ca^{2+} intensity versus BC area (B) in cells treated with GsMTx-4. Arrows in (A) and (B) indicate BCV formation. (C) Time-lapse phase-contrast and Ca^{2+} images of cells treated with GsMTx-4, red arrows indicate BCV. Scale bar represents 10 μm. (D) Kymographs from six different BCs from three independent experiments from cells treated with GsMTx-4. Yellow arrowheads indicate BCV. (E) Quantification of BCV frequency (n = 30, 3 independent experiments). (F) Model for GsMTx-4 mediated Piezo-1 inhibition and induced BCV formation. When BC expands in presence of GsMTx-4, Piezo-1 is inhibited and remains inactive, and Ca^{2+} is trapped inside BC. Increasing canalicular pressure causes localized rupture of the actomyosin cortex, leading to canalicular membrane protruding into cell and detaching itself from BC membrane, giving rise to BCV. (For interpretation of the references to color in this figure legend, the reader is referred to the Web version of this article.)

and drug-induced hepatocellular cholestasis.

We adopted collagen sandwich culture of primary rat hepatocytes, which exhibits appreciable BC with periodic contractions. Using live Ca^{2+} markers, we found that BC had high levels of Ca^{2+}. Various active Ca^{2+} channels have already been identified that mediate Ca^{2+} entry into the BC [41]. Here, we found that BC-Ca^{2+} fluctuated periodically in coherence with the contractions. Previous studies of Ca^{2+} waves in hepatocytes were performed near the cell-substrate [9] contact plane using either TIRF or confocal imaging, and BC Ca^{2+} was not observed in such studies. The Ca^{2+} visualization requires either wide-field imaging or

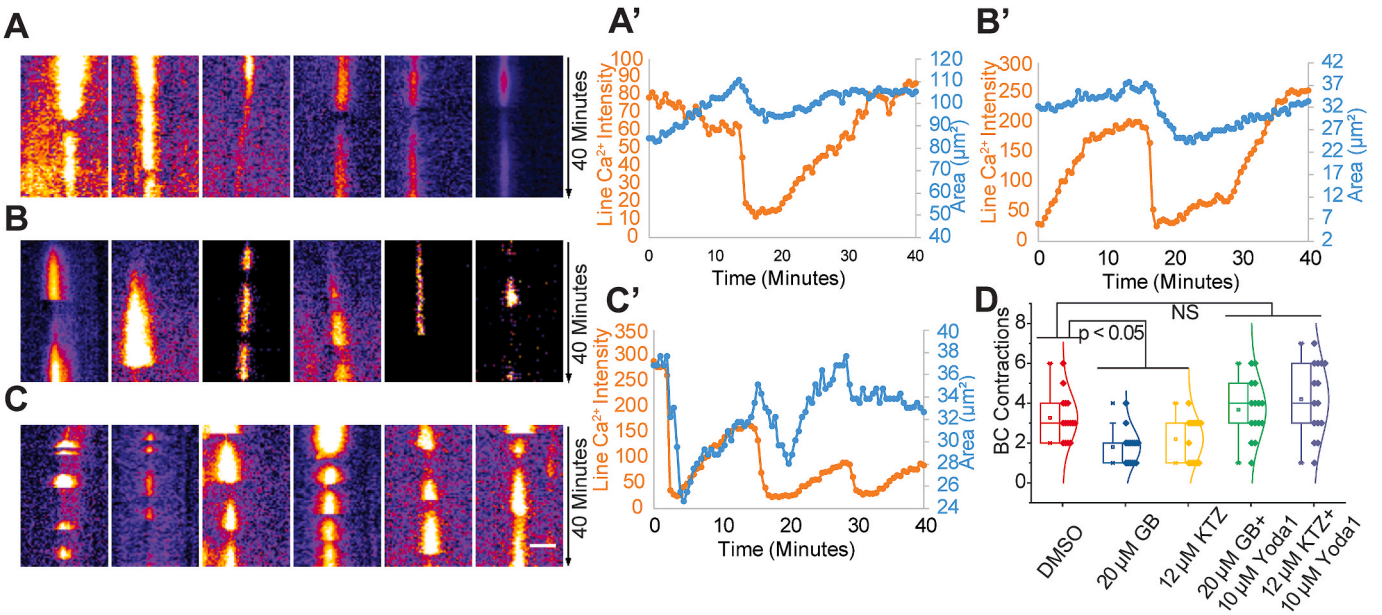

Fig. 7. Piezo-1 activation rescues BC contractility in drug induced hepatocellular cholestasis. Kymographs for six different BCs from three independent experiments for cells treated with Glyburide (GB) (A) and Ketoconazole (KTZ) (B). (A′) and (B′) Graphs represent BC line Ca^{2+} intensity and the BC area in cells treated with GB and KTZ respectively. (C) Kymographs for six different BCs from three independent experiments for cells treated with GB and Yoda-1. Representative graph of BC line Ca^{2+} intensity versus BC area in cells under the same treatment (C′). (D) Quantification of BC contractions in 40 min under the aforementioned treatments and KTZ + Yoda1 showing that BC contractility is reduced in presence of MRP-2 and BSEP inhibitors and it can be rescued using Yoda-1. N = 15, five each from three independent experiments.

confocal imaging at ~2–4 μm above the cell-substrate contact plane, since BC is lumenal and is located ~1.5 μm above the cell-substrate contact plane. High-resolution temporal imaging showed that depletion of BC Ca^{2+} preceded the contractions. Concurrently, intracellular Ca^{2+} increased with every BC contraction. Since intracellular Ca^{2+} surges can drive PAC contractility [7,15,42,43], we speculate trafficking of Ca^{2+} from BC into hepatocytes triggers PAC contractions and hence, BC contractions. Our previous work elucidated the impact of ICP on PAC contractility. Considering the pressure-driven nature of BC contractions, and Ca^{2+} transport across the BC membrane, we hypothesized a pressure-sensitive Ca^{2+} channel to be involved in this process. We screened for four major MCCs and found Piezo-1 to be localized on the BC membrane. This does not exclude the involvement of lesser-known MCCs, such as transmembrane channel-like protein-1, which could potentially affect Ca^{2+} transport across the BC. The activation and inhibition of Piezo-1 by Yoda-1 and GsMTX-4 [35,44] increases and decreases BC contractions respectively, suggests that Piezo-1 controls BC dynamics.

The finding that the MCC, Piezo-1 responds to the canalicular pressure and controls the intracellular Ca^{2+} trafficking has three main implications. First, this mechanism allows autonomous control of the BC dynamics, which obviates the need for external triggers such as hormones and growth factors for BC contractions [4,45]. This would allow the BC to contract as and when the threshold ICP is reached, as the lumen cannot tolerate limitless expansion. Secondly, it explains the cholestatic effects of drugs that inhibit BC transporters such as BSEP and MRP2 [46,47]. BSEP (ABC11) is involved in secreting monovalent BA such as taurine or glycine-amidates of cholic acid into BC [48,49]. Bilirubin, another major component of bile is secreted via MRP2 (ABC 2) [50]. MRP2 is also responsible for the secretion of various organic anions formed by phase 2 conjugation and divalent BA. BSEP and MRP2 secretions increase the osmolality inside BC, commencing water movement into BC via aquaporins [51] and thereby increasing ICP [52]. When the activity of these transporters is inhibited [2], there is reduced lumenal contents in the BC and decreased ICP, insufficient for the activation of Piezo-1 and BC contractions. The decrease in BC contractions leads to the stasis of the bile in the lumen.

Thirdly, the interplay between the transporter activity and mechano-activation of the ion channel opens the possibility of Piezo-1 manipulation to restore BC dynamics in acute hepatocellular cholestasis. Blocking transporter activity using GB and KTZ led to reduced BC contractions, corroborating the idea that efficient transporter activity is required for BC contractions. BC contractility was restored when Piezo-1 was activated using Yoda-1, which hyper-sensitizes Piezo-1 to lower ICP. This mechanism could be exploited as an adjuvant therapeutic strategy to improve BC contractions in acute hepatocellular cholestasis. Further studies are required to explore the feasibility of this approach in chronic cholestasis wherein multiple feedback mechanisms are operational [53,54].

Our study elucidates the long-debated mechanism of BC contractions. Although the involvement of Ca^{2+} in mediating BC contractions had been shown decades ago, a clear mechanistic explanation had not been provided. Our study is the first to investigate the involvement of an MCC in the contraction of the BC lumen. The Piezo channels have been implicated in sensing light, touch and proprioception, compressive forces in chondrocytes, substrate stiffness in neuronal differentiation, shear stress and regulation of vascular branching, and, fluid flow in nephrons [55–59]. Our data has extended the functionality of the Piezo channels to sensing canalicular pressure and regulating BC contractions. Our work also raises the possibility of using Ca^{2+} imaging as surrogate readout for BC contractions. Taken together, the understanding of the BC dynamics offers possibilities to develop effective treatment strategies for hepatocellular cholestasis.

Deregulation of Piezo-1 expression has been implicated in liver diseases. Recently Zhao et al., have shown a correlation of hepatic steatosis and Piezo-1 expression in adipose tissue [60]. Piezo-1 is overexpressed in liver cancer [61]. Ca^{2+} signaling modulates diverse liver functions and is implicated in normal physiology and liver diseases [20]. Ca^{2+} regulation via Piezo-1 could be further explored to uncover new insights in mechanosensing in liver regeneration [62,63]. Furthermore, MCC have been known to play a major role in regulating endothelial lumen dynamics [58,64] by sensing intra-vascular pressure [65]. However, the

role of MCC in secretion-driven pressure in secretory lumens (such as acini, canaliculi, blastocysts) has not been studied in detail. Here, we have shown an example of a secretary lumen, BC, and proposed a mechanism wherein MCC senses secretion-driven pressure to regulate lumen dynamics. Further studies are required to uncover similar mechanisms that might be involved in regulating the dynamics of other secretory lumens wherein pressure sensing is central to tissue functionality [66].

Data availability

The authors declare that all data supporting the findings of this study are available within the paper (and its supplementary information files). Correspondance and requests for materials should be addressed to H.Y. and B.C.L.

Financial support

We acknowledge funding support from the Mechanobiology Institute (National University of Singapore, Singapore, Grant number: R-714-006-008-271), Institute of Bioengineering and Nanotechnology, Biomedical Research Council IAF-PP (A*STAR, Singapore), NUHS Innovation Seed Grant 2017 (R-185-000-343-733); CAMP, Singapore-MIT Alliance for Research and Technology; National Medical Research Council (Ministry of Health, Singapore, Grant Number: R-185-000-294-511) and MOE ARC (R-185-000-342-112) to HY. LTK and BPN were supported by the Singapore Ministry of Health's National Medical Research Council (NMRC) under its Open Fund Individual Research Grant scheme (NMRC/OFIRG/0007/2016). KG was supported by MBI scholarship.

CRediT authorship contribution statement

Kapish Gupta: Conceptualization, Formal analysis, Methodology, Investigation, Writing - original draft. **Inn Chuan Ng:** Formal analysis, Methodology. **Gowri Manohari Balachander:** Formal analysis, Methodology, Writing - review & editing. **Binh P. Nguyen:** Methodology. **Lisa Tucker-Kellogg:** Methodology, Writing - review & editing. **Boon Chuan Low:** Conceptualization, Resources, Funding acquisition, Supervision, Writing - review & editing. **Hanry Yu:** Conceptualization, Resources, Funding acquisition, Supervision, Writing - review & editing.

Declaration of competing interest

Hanry Yu declares holding equity in Invitrocue, Osteopore, Histoindex, Vasinfuse and Pishon biomedical that have no conflict of interest with the work reported in this paper.

Acknowledgements

Diego Pitta de Araujo, Animator, Science Communications Core, Mechanobiology Institute, National University of Singapore designed all the animations. Hui Ting, Image Processing Core, Mechanobiology Institute helped with image processing. We also thank the Microscopy Core at the Mechanobiology Institute, and NUHS core facilities, National University of Singapore for their help with microscopy. KG is a Mechanobiology Institute PhD scholar.

Appendix A. Supplementary data

Supplementary data to this article can be found online at https://doi.org/10.1016/j.biomaterials.2020.120283.

References

[1] M. Trauner, P.J. Meier, J.L. Boyer, Molecular pathogenesis of cholestasis, N. Engl. J. Med. 339 (17) (1998) 1217–1227.
[2] M.S. Padda, M. Sanchez, A.J. Akhtar, J.L. Boyer, Drug-induced cholestasis, Hepatology 53 (4) (2011) 1377–1387.
[3] C. Pauli-Magnus, P.J. Meier, Hepatocellular transporters and cholestasis, J. Clin. Gastroenterol. 39 (4 Suppl 2) (2005) S103–S110.
[4] N. Watanabe, N. Tsukada, C.R. Smith, M.J. Phillips, Motility of bile canaliculi in the living animal: implications for bile flow, J. Cell Biol. 113 (5) (1991) 1069–1080.
[5] P.L. Jansen, A. Ghallab, N. Vartak, R. Reif, F.G. Schaap, J. Hampe, J.G. Hengstler, The ascending pathophysiology of cholestatic liver disease, Hepatology (Baltimore, Md 65 (2) (2017) 722–738.
[6] N. Watanabe, T. Kagawa, S. Kojima, S. Takashimizu, N. Nagata, Y. Nishizaki, T. Mine, Taurolithocholate impairs bile canalicular motility and canalicular bile secretion in isolated rat hepatocyte couplets, World J. Gastroenterol. 12 (33) (2006) 5320–5325.
[7] A. Sharanek, A. Burban, M. Burbank, R. Le Guevel, R. Li, A. Guillouzo, C. Guguen-Guillouzo, Rho-kinase/myosin light chain kinase pathway plays a key role in the impairment of bile canaliculi dynamics induced by cholestatic drugs, Sci. Rep. 6 (2016) 24709.
[8] S. Watanabe, M. Tomono, M. Takeuchi, T. Kitamura, M. Hirose, A. Miyazaki, T. Namihisa, Bile canalicular contraction in the isolated hepatocyte doublet is related to an increase in cytosolic free calcium ion concentration, Liver 8 (3) (1988) 178–183.
[9] J. Nagata, M.T. Guerra, C.A. Shugrue, D.A. Gomes, N. Nagata, M.H. Nathanson, Lipid rafts establish calcium waves in hepatocytes, Gastroenterology 133 (1) (2007) 256–267.
[10] M.H. Nathanson, A.D. Burgstahler, A. Mennone, M.B. Fallon, C.B. Gonzalez, J. C. Saez, Ca2+ waves are organized among hepatocytes in the intact organ, Am. J. Physiol. 269 (1 Pt 1) (1995) G167–G171.
[11] B. Bouscarel, H. Fromm, R. Nussbaum, Ursodeoxycholate mobilizes intracellular Ca2+ and activates phosphorylase a in isolated hepatocytes, Am. J. Physiol. 264 (2 Pt 1) (1993) G243–G251.
[12] K. Gupta, Q. Li, J.J. Fan, E.L.S. Fong, Z. Song, S. Mo, H. Tang, I.C. Ng, C.W. Ng, P. Pawijit, S. Zhuo, C.Y. Dong, B.C. Low, A. Wee, Y.Y. Dan, P. Kanchanawong, P. So, V. Viasnoff, H. Yu, Actomyosin contractility drives bile regurgitation as an early response during obstructive cholestasis, J. Hepatol. 66 (6) (2017) 1231–1240.
[13] X. Luo, K. Gupta, A. Ananthanarayanan, Z. Wang, L. Xia, A. Li, R.B. Sakban, S. Liu, H. Yu, Directed differentiation of adult liver derived mesenchymal like stem cells into functional hepatocytes, Sci. Rep. 8 (1) (2018) 2818.
[14] I.M. Arias, M. Che, Z. Gatmaitan, C. Leveille, T. Nishida, M. St Pierre, The biology of the bile canaliculus, Hepatology (Baltimore, Md 17 (2) (1993) 318–329.
[15] M.G. Burbank, A. Burban, A. Sharanek, R.J. Weaver, C. Guguen-Guillouzo, A. Guillouzo, Early alterations of bile canaliculi dynamics and the Rho kinase/myosin light chain kinase pathway are characteristics of drug-induced intrahepatic cholestasis, Drug Metab. Dispos. 44 (11) (2016) 1780–1793.
[16] Q. Li, Y. Zhang, P. Pluchon, J. Robens, K. Herr, M. Mercade, J.P. Thiery, H. Yu, V. Viasnoff, Extracellular matrix scaffolding guides lumen elongation by inducing anisotropic intercellular mechanical tension, Nat. Cell Biol. 18 (3) (2016) 311–318.
[17] R. Reif, J. Karlsson, G. Gunther, L. Beattie, D. Wrangborg, S. Hammad, B. Begher-Tibbe, A. Vartak, S. Melega, P.M. Kaye, J.G. Hengstler, M. Jirstrand, Bile canalicular dynamics in hepatocyte sandwich cultures, Arch. Toxicol. 89 (10) (2015) 1861–1870.
[18] J. Akerboom, T.W. Chen, T.J. Wardill, L. Tian, J.S. Marvin, S. Mutlu, N. C. Calderon, F. Esposti, B.G. Borghuis, X.R. Sun, A. Gordus, M.B. Orger, R. Portugues, F. Engert, J.J. Macklin, A. Filosa, A. Aggarwal, R.A. Kerr, R. Takagi, S. Kracun, E. Shigetomi, B.S. Khakh, H. Baier, L. Lagnado, S.S. Wang, C. I. Bargmann, B.E. Kimmel, V. Jayaraman, K. Svoboda, D.S. Kim, E.R. Schreiter, L. L. Looger, Optimization of a GCaMP calcium indicator for neural activity imaging, J. Neurosci. 32 (40) (2012) 13819–13840.
[19] R. Bagur, G. Hajnoczky, Intracellular Ca(2+) sensing: its role in calcium homeostasis and signaling, Mol. Cell 66 (6) (2017) 780–788.
[20] M.J. Amaya, M.H. Nathanson, Calcium signaling in the liver, Comprehensive Physiology 3 (1) (2013) 515–539.
[21] M. Wictome, I. Henderson, A.G. Lee, J.M. East, Mechanism of inhibition of the calcium pump of sarcoplasmic reticulum by thapsigargin, Biochem. J. 283 (Pt 2) (1992) 525–529.
[22] C.M. Oslowski, F. Urano, Chapter four - measuring ER stress and the unfolded protein response using mammalian tissue culture system, in: P.M. Conn (Ed.), Methods in Enzymology, Academic Press2011, pp. 71-92.
[23] G. Grigoryan, M. Segal, Prenatal stress alters noradrenergic modulation of LTP in hippocampal slices, J. Neurophysiol. 110 (2) (2013) 279–285.
[24] Y. Komori, M. Tanaka, M. Kuba, M. Ishii, M. Abe, N. Kitamura, A. Verkhratsky, I. Shibuya, G. Dayanithi, Ca(2+) homeostasis, Ca(2+) signalling and somatodendritic vasopressin release in adult rat supraoptic nucleus neurones, Cell Calcium 48 (6) (2010) 324–332.
[25] E. Krause, F. Pfeiffer, A. Schmid, I. Schulz, Depletion of intracellular calcium stores activates a calcium conducting nonselective cation current in mouse pancreatic acinar cells, J. Biol. Chem. 271 (51) (1996) 32523–32528.
[26] E.J. Nelson, C.C. Li, R. Bangalore, T. Benson, R.S. Kass, P.M. Hinkle, Inhibition of L-type calcium-channel activity by thapsigargin and 2,5-t-butylhydroquinone, but not by cyclopiazonic acid, Biochem. J. 302 (Pt 1) (1994) 147–154.

[27] S. Miyamoto, M. Izumi, M. Hori, M. Kobayashi, H. Ozaki, H. Karaki, Xestospongin C, a selective and membrane-permeable inhibitor of IP(3) receptor, attenuates the positive inotropic effect of alpha-adrenergic stimulation in Guinea-pig papillary muscle, Br. J. Pharmacol. 130 (3) (2000) 650–654.
[28] J. Gafni, J.A. Munsch, T.H. Lam, M.C. Catlin, L.G. Costa, T.F. Molinski, I.N. Pessah, Xestospongins: potent membrane permeable blockers of the inositol 1,4,5-trisphosphate receptor, Neuron 19 (3) (1997) 723–733.
[29] H. Ozaki, M. Hori, Y.S. Kim, S.C. Kwon, D.S. Ahn, H. Nakazawa, M. Kobayashi, H. Karaki, Inhibitory mechanism of xestospongin-C on contraction and ion channels in the intestinal smooth muscle, Br. J. Pharmacol. 137 (8) (2002) 1207–1212.
[30] S. Watanabe, M. Tomono, M. Takeuchi, T. Kitamura, M. Hirose, A. Miyazaki, T. Namihisa, Bile canalicular contraction in the isolated hepatocyte doublet is related to an increase in cytosolic free calcium ion concentration, Liver 8 (3) (2008) 178–183.
[31] T. Przygodzki, A. Sokal, M. Bryszewska, Calcium ionophore A23187 action on cardiac myocytes is accompanied by enhanced production of reactive oxygen species, Biochim. Biophys. Acta 1740 (3) (2005) 481–488.
[32] B. Martinac, Mechanosensitive ion channels: molecules of mechanotransduction, J. Cell Sci. 117 (Pt 12) (2004) 2449–2460.
[33] P. Ridone, E. Pandzic, M. Vassalli, C.D. Cox, A. Macmillan, P.A. Gottlieb, B. Martinac, Disruption of Membrane Cholesterol Organization Impairs the Concerted Activity of PIEZO1 Channel Clusters, bioRxiv, 2019, p. 604488.
[34] C.D. Cox, P.A. Gottlieb, Amphipathic molecules modulate PIEZO1 activity, Biochem. Soc. Trans. 47 (6) (2019) 1833–1842.
[35] C. Bae, F. Sachs, P.A. Gottlieb, The mechanosensitive ion channel Piezo1 is inhibited by the peptide GsMTx4, Biochemistry 50 (29) (2011) 6295–6300.
[36] C. Gedeon, J. Behravan, G. Koren, M. Piquette-Miller, Transport of glyburide by placental ABC transporters: implications in fetal drug exposure, Placenta 27 (11–12) (2006) 1096–1102.
[37] J. Zhang, K. He, L. Cai, Y.C. Chen, Y. Yang, Q. Shi, T.F. Woolf, W. Ge, L. Guo, J. Borlak, W. Tong, Inhibition of bile salt transport by drugs associated with liver injury in primary hepatocytes from human, monkey, dog, rat, and mouse, Chem. Biol. Interact. 255 (2016) 45–54.
[38] E.S. Bjornsson, J.G. Jonasson, Drug-induced cholestasis, Clin. Liver Dis. 17 (2) (2013) 191–209.
[39] M. Wagner, G. Zollner, M. Trauner, New molecular insights into the mechanisms of cholestasis, J. Hepatol. 51 (3) (2009) 565–580.
[40] B. Stieger, K. Fattinger, J. Madon, G.A. Kullak-Ublick, P.J. Meier, Drug- and estrogen-induced cholestasis through inhibition of the hepatocellular bile salt export pump (Bsep) of rat liver, Gastroenterology 118 (2) (2000) 422–430.
[41] H. Yokomori, M. Oda, Y. Kamegaya, M. Ogi, N. Tsukada, H. Ishii, Bile canalicular contraction and dilatation in primary culture of rat hepatocytes – possible involvement of two different types of plasma membrane Ca2+-Mg2+-ATPase and Ca2+-pump-ATPase, Med. Electron. Microsc. 34 (2) (2001) 115–122.
[42] E.L. LeCluyse, J.A. Fix, K.L. Audus, J.H. Hochman, Regeneration and maintenance of bile canalicular networks in collagen-sandwiched hepatocytes, Toxicol. Vitro : an international journal published in association with BIBRA 14 (2) (2000) 117–132.
[43] R. Sudo, H. Kohara, T. Mitaka, M. Ikeda, K. Tanishita, Coordinated movement of bile canalicular networks reconstructed by rat small hepatocytes, Ann. Biomed. Eng. 33 (5) (2005) 696–708.
[44] R. Syeda, M.N. Florendo, C.D. Cox, J.M. Kefauver, J.S. Santos, B. Martinac, A. Patapoutian, Piezo1 channels are inherently mechanosensitive, Cell Rep. 17 (7) (2016) 1739–1746.
[45] S. Watanabe, M.J. Phillips, Ca2+ causes active contraction of bile canaliculi: direct evidence from microinjection studies, Proc. Natl. Acad. Sci. U.S.A. 81 (19) (1984) 6164–6168.
[46] F. Yang, T. Takeuchi, K. Tsuneyama, T. Yokoi, S. Oda, Experimental evidence of liver injury by BSEP-inhibiting drugs with a bile salt supplementation in rats, Toxicol. Sci. 170 (1) (2019) 95–108.
[47] L. Payen, L. Delugin, A. Courtois, Y. Trinquart, A. Guillouzo, O. Fardel, The sulphonylurea glibenclamide inhibits multidrug resistance protein (MRP1) activity in human lung cancer cells, Br. J. Pharmacol. 132 (3) (2001) 778–784.
[48] J.A. Byrne, S.S. Strautnieks, G. Mieli-Vergani, C.F. Higgins, K.J. Linton, R. J. Thompson, The human bile salt export pump: characterization of substrate specificity and identification of inhibitors, Gastroenterology 123 (5) (2002) 1649–1658.
[49] H. Hayashi, T. Takada, H. Suzuki, R. Onuki, A.F. Hofmann, Y. Sugiyama, Transport by vesicles of glycine- and taurine-conjugated bile salts and taurolithocholate 3-sulfate: a comparison of human BSEP with rat Bsep, Biochim. Biophys. Acta 1738 (1–3) (2005) 54–62.
[50] D. Keppler, The roles of MRP2, MRP3, OATP1B1, and OATP1B3 in conjugated hyperbilirubinemia, Drug Metab. Dispos. 42 (4) (2014) 561–565.
[51] P. Portincasa, A. Moschetta, A. Mazzone, G. Palasciano, M. Svelto, G. Calamita, Water handling and aquaporins in bile formation: recent advances and research trends, J. Hepatol. 39 (5) (2003) 864–874.
[52] S. Dasgupta, K. Gupta, Y. Zhang, V. Viasnoff, J. Prost, Physics of lumen growth, Proc. Natl. Acad. Sci. U.S.A. 115 (21) (2018) E4751–E4757.
[53] H. Hyogo, S. Tazuma, T. Nishioka, H. Ochi, A. Yamaguchi, Y. Numata, K. Kanno, M. Sakomoto, Y. Asamoto, K. Tsuboi, K. Nakai, S. Yasumiba, Y. Sunami, G. Kajiyama, Phospholipid alterations in hepatocyte membranes and transporter protein changes in cholestatic rat model, Dig. Dis. Sci. 46 (10) (2001) 2089–2097.
[54] G. Zollner, P. Fickert, D. Silbert, A. Fuchsbichler, H.-U. Marschall, K. Zatloukal, H. Denk, M. Trauner, Adaptive changes in hepatobiliary transporter expression in primary biliary cirrhosis, J. Hepatol. 38 (6) (2003) 717–727.
[55] A.T. Chesler, M. Szczot, Portraits of a pressure sensor, Elife 7 (2018), e34396.
[56] B. Rode, J. Shi, N. Endesh, M.J. Drinkhill, P.J. Webster, S.J. Lotteau, M.A. Bailey, N.Y. Yuldasheva, M.J. Ludlow, R.M. Cubbon, J. Li, T.S. Futers, L. Morley, H. J. Gaunt, K. Marszalek, H. Viswambharan, K. Cuthbertson, P.D. Baxter, R. Foster, P. Sukumar, A. Weightman, S.C. Calaghan, S.B. Wheatcroft, M.T. Kearney, D. J. Beech, Piezo1 channels sense whole body physical activity to reset cardiovascular homeostasis and enhance performance, Nat. Commun. 8 (1) (2017) 350.
[57] S.S. Ranade, Z. Qiu, S.H. Woo, S.S. Hur, S.E. Murthy, S.M. Cahalan, J. Xu, J. Mathur, M. Bandell, B. Coste, Y.S. Li, S. Chien, A. Patapoutian, Piezo1, a mechanically activated ion channel, is required for vascular development in mice, Proc. Natl. Acad. Sci. U.S.A. 111 (28) (2014) 10347–10352.
[58] W.A. AbouAlaiwi, M. Takahashi, B.R. Mell, T.J. Jones, S. Ratnam, R.J. Kolb, S. M. Nauli, Ciliary polycystin-2 is a mechanosensitive calcium channel involved in nitric oxide signaling cascades, Circ. Res. 104 (7) (2009) 860–869.
[59] J. Wu, A.H. Lewis, J. Grandl, Touch, tension, and transduction - the function and regulation of Piezo ion channels, Trends Biochem. Sci. 42 (1) (2017) 57–71.
[60] C. Zhao, Q. Sun, L. Tang, Y. Cao, J.L. Nourse, M.M. Pathak, X. Lu, Q. Yang, Mechanosensitive ion channel Piezo1 regulates diet-induced adipose inflammation and systemic insulin resistance, Front. Endocrinol. 10 (373) (2019).
[61] K. Nonomura, V. Lukacs, D.T. Sweet, L.M. Goddard, A. Kanie, T. Whitwam, S. S. Ranade, T. Fujimori, M.L. Kahn, A. Patapoutian, Mechanically activated ion channel PIEZO1 is required for lymphatic valve formation, Proc. Natl. Acad. Sci. Unit. States Am. 115 (50) (2018) 12817–12822.
[62] Z. Song, K. Gupta, I.C. Ng, J. Xing, Y.A. Yang, H. Yu, Mechanosensing in liver regeneration, Semin. Cell Dev. Biol. 71 (2017) 153–167.
[63] K. Gupta, Z. Song, H. Tang, E.L.S. Fong, I.C. Ng, H. Yu, 6.28 liver tissue Engineering☆, in: P. Ducheyne (Ed.), Comprehensive Biomaterials II, Elsevier, Oxford, 2017, pp. 491–512.
[64] D. Guo, S. Liang, S. Wang, C. Tang, B. Yao, W. Wan, H. Zhang, H. Jiang, A. Ahmed, Z. Zhang, Y. Gu, Role of epithelial Na+ channels in endothelial function, J. Cell Sci. 129 (2) (2016) 290–297.
[65] H.J. Knot, M.T. Nelson, Regulation of arterial diameter and wall [Ca2+] in cerebral arteries of rat by membrane potential and intravascular pressure, J. Physiol. 508 (Pt 1) (1998) 199–209.
[66] J.L. Pluznick, M.J. Caplan, Chemical and physical sensors in the regulation of renal function, Clin. J. Am. Soc. Nephrol. 10 (9) (2015) 1626–1635.